

AUTOMATIC SEGMENTATION AND 3D VISUALIZATION OF MR IMAGES

OF PELVIC FLOOR

Javier A. Salazar¹

Joint work with Gaik Ambartsoumian¹, Gaurav Khatri², and Philippe Zimmern³

Department of Mathematics¹, University of Texas at Arlington, Arlington, TX
 Departments of Radiology² and Urology³, University of Texas Southwestern Medical Center, Dallas, TX

Introduction

Pelvic floor disorders, which include pelvic organ prolapse (POP), affect nearly 1 in 4 women in the US [7]. Each year more than 300,000 surgical procedures are performed in the US just for POP alone [8]. Most common surgical repair procedures of pelvic floor include placement of synthetic implants such as urethral slings and vaginal meshes. Unfortunately, post-operative complications of these procedures (e.g. dyspareunia, chronic pain, extrusion, or recurrent infection) are not rare, and their treatment may require follow-up surgeries to remove the implants. In these cases, imaging of the pelvic floor is a vital necessity for surgeons planning the procedure, seeking to identify the implants, their relative location and distance from various organs. The process is further complicated by the poor contrast between the implants and scar tissue, as well as the need for the surgeon to mentally visualize a 3D volumetric image from 2D projections generated by standard MRI. This work aims to address some of these issues and assist surgeons by improving the currently available imaging techniques. In particular, we study the possibility of using multi-atlas segmentation (MAS) to automatically segment 2D MR images of pelvic floor, as well as utilizing such segmentations to create 3D semi-transparent volumetric images that can be rotated and zoomed with a mouse on the computer screen.

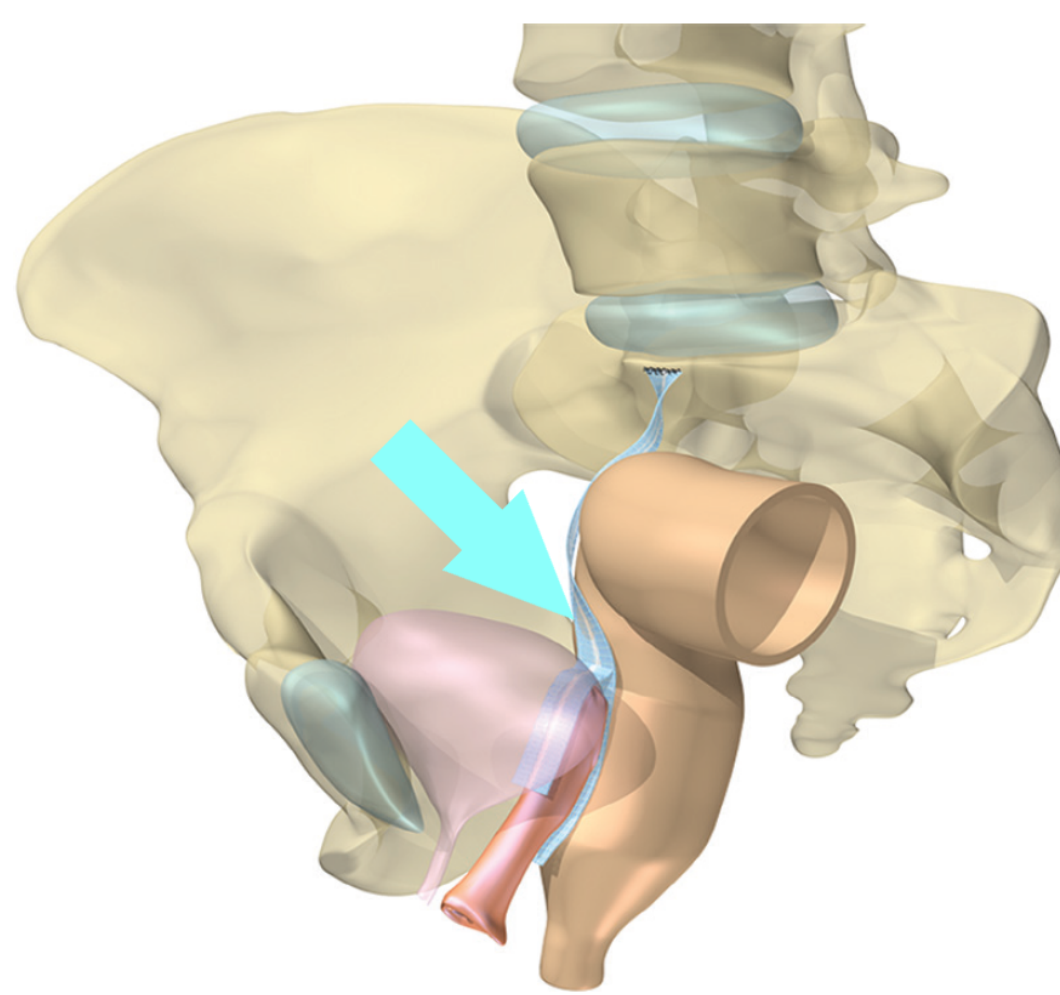


Fig. 1: Illustration of SC mesh (cyan arrow) shown relative to pelvic floor (from [6]).

In the illustration shown above, we can see an example of a mesh placed from sacral promontory to vaginal apex in order to correct vaginal apex or uterocervical prolapse. In the figure below, we can see a sagittal MRI slice with the SC mesh shown from Fig. 1 near the cyan arrow along with important pelvic organs. As one can detect, it is difficult to see the full SC mesh from one sagittal slice. Typically, the doctors will analyze all of the axial, coronal, and sagittal slices to form a mental picture of how the mesh is located and oriented in the body to plan for removal.

This research aims at providing surgeons and radiologists 3D visualization tools for pelvic floor organs and synthetic implants. Thus, this does not only provide a second opinion regarding mesh/sling placement and orientation but assists in easier surgical planning coordination between radiologists and surgeons.

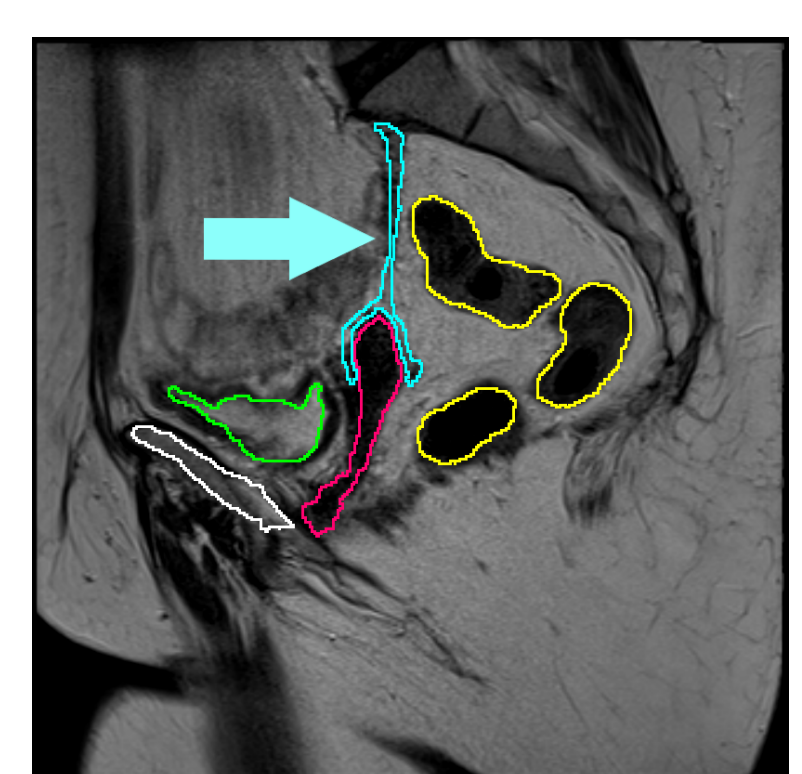


Fig. 2: Manually segmented, sagittal MRI slice with SC mesh (cyan) shown along with vagina (red), bladder (green), bowel (yellow), and pubic bone (white).

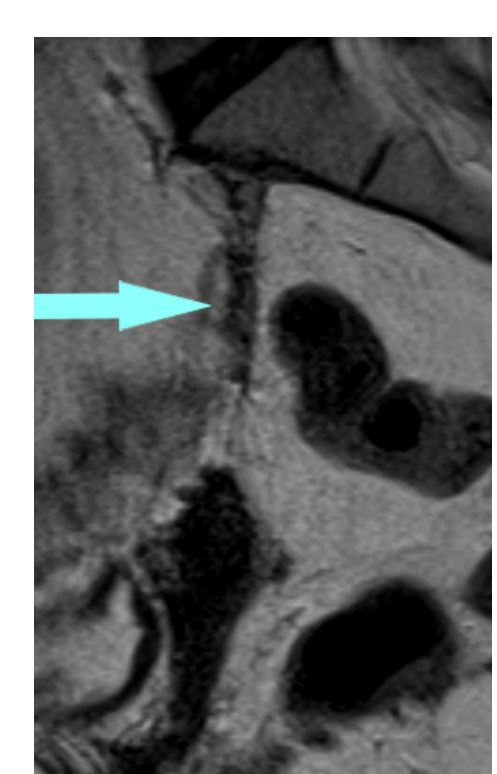


Fig. 3: A closeup of the SC mesh near the cyan arrow without any outlines blocking the view.

Multi-Atlas Segmentation (MAS)

MAS consists of three parts known as image registration, label propagation, and label fusion [5]. In image registration, we use optimization theory to find a transformation between labeled MRI slices from the patient data set and the unlabeled MRI slices from a new patient. In the figures below, we see an example of image registration using a deformable model known as Symmetric Normalization (SyN) [4] implemented using open source software "Advanced Normalization Tools (ANTS)" [3]. Moreover, ANTs is used for the label propagation and label fusion processes as well. Notice how features, such as the bladder, from Fig. 4 have been stretched in Fig. 8 to match the features in Fig. 6.



Fig. 4: MR image in the axial orientation from the manually segmented data set.

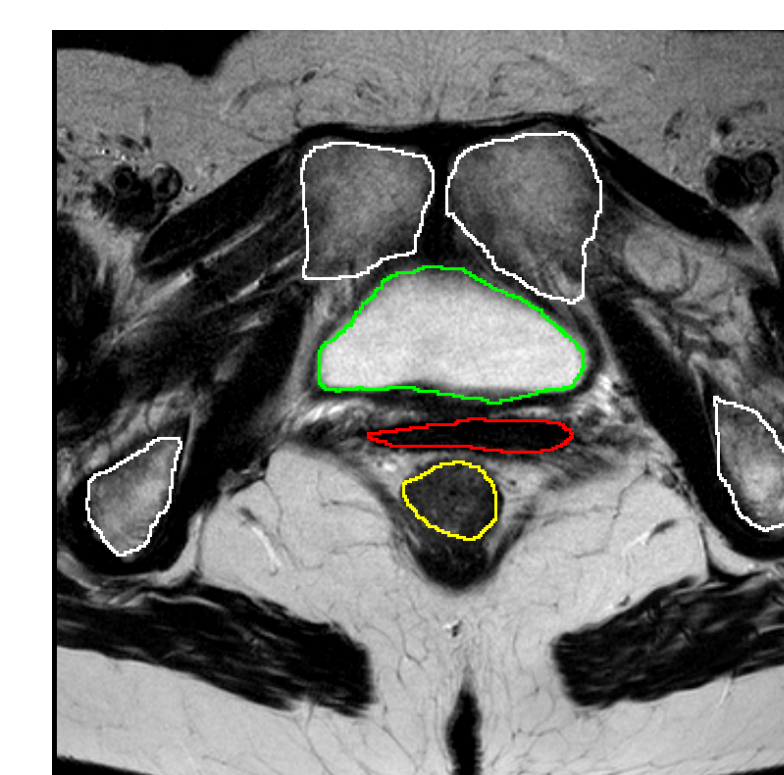


Fig. 5: Manually segmented labels from Fig. 4 MRI slice.

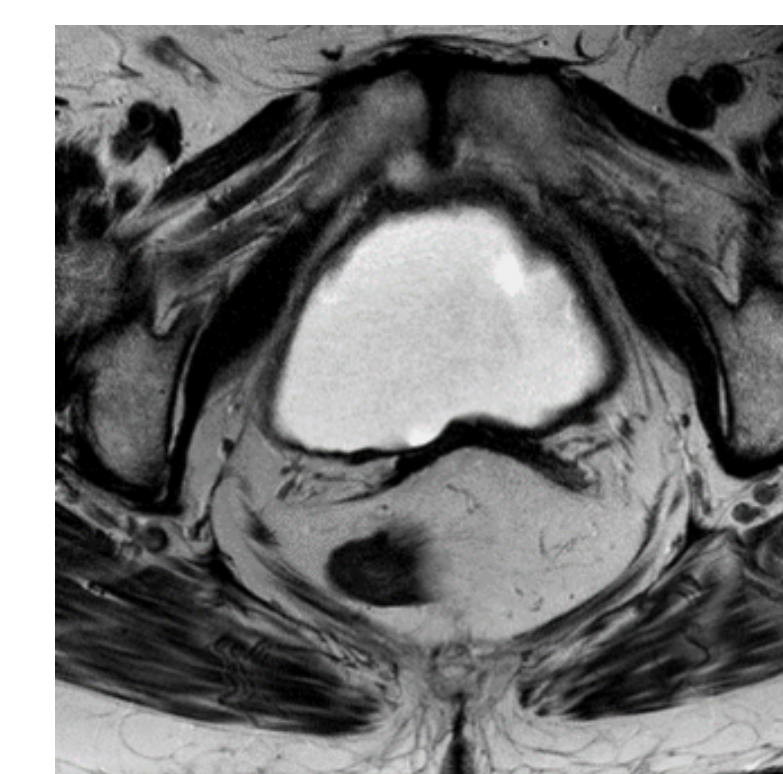


Fig. 6: MR image in the axial orientation from a new patient.

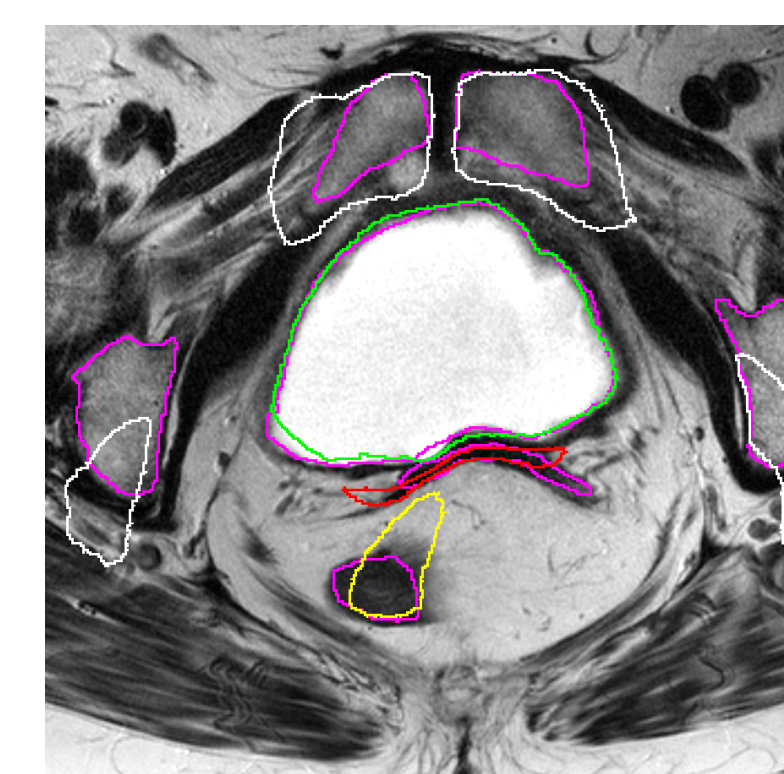


Fig. 7: Automatically segmented labels from Fig. 6 MRI slice using image registration.
 "Truth" data shown in magenta for comparison.



Fig. 8: Transformed Fig. 4 image using the SyN deformable model to closely match Fig. 6 image.

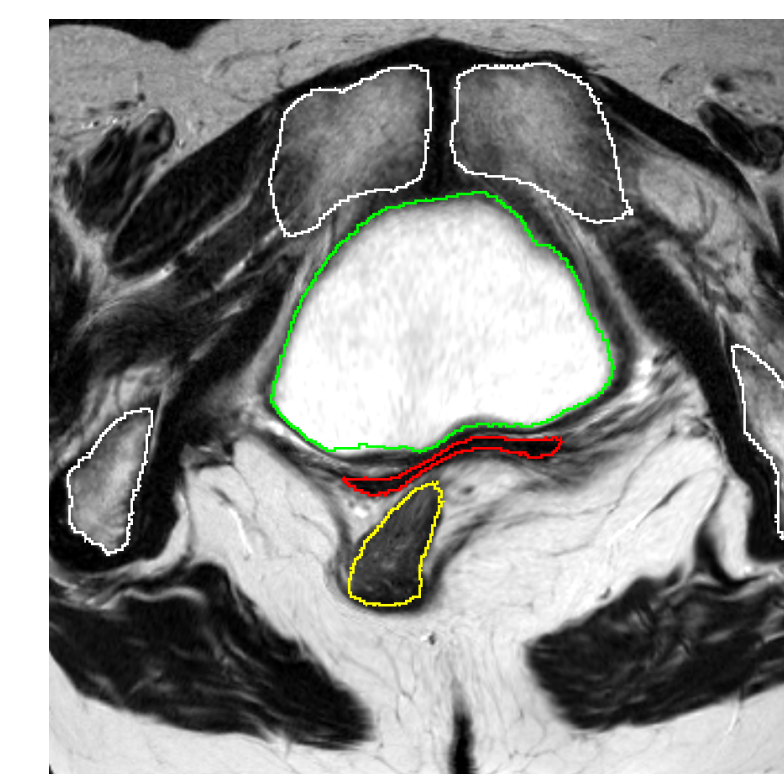


Fig. 9: Propagated labels from Fig. 5 MRI slice using the found transformation.

Once this is done, we can propagate the labels from the transformed known data from many patients onto the new patient. In Fig. 10, one can see multiple labels per organ propagated to this previously unlabeled slice. There is variability between labels since no two patients are exactly the same. Patients can be taller or shorter, overweight or underweight, and rotated differently in MRI machines thus leading to different location and size of pelvic organs. The image registration process reduces the variability between patients by minimizing the differences between the two images under a transformation model.

Finally, the image fusion process will merge all of the labels into only one label per organ. A simple way to do this, for example, is to accept locations where there is 80% agreement among labels and reject elsewhere; this is known as Majority Voting (MV). In this case, we are using Joint Label Fusion (JLF) [9] to handle this process. The advantage of JLF over MV is that not only we look at correlation among labels but the unlabeled image itself is used as well to guide the fusion process. Thus, edge information from the unlabeled image can help fix abnormalities among label information. In Fig. 11, one can notice the results of performing label fusion from Fig. 10. Once this is done on multiple slices, we can use 3D visualization software as shown in Fig. 12 below to assist radiologists and surgeons in surgical planning.

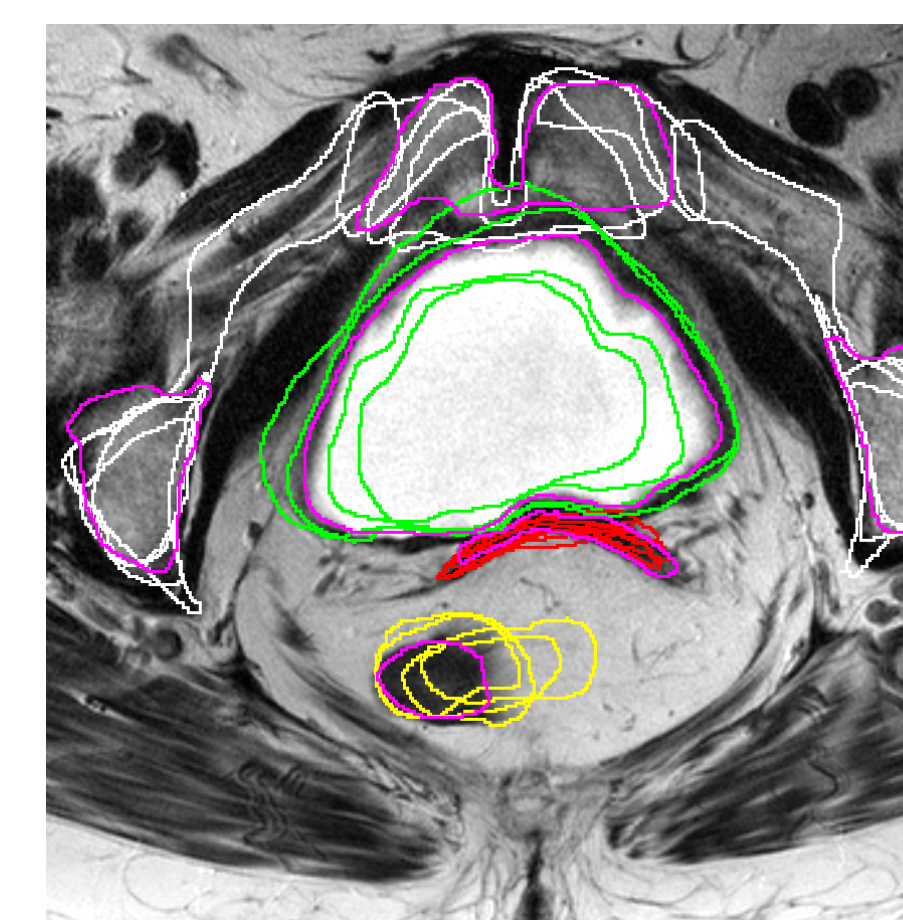


Fig. 10: Propagated labels on unlabeled slice from Fig. 6.

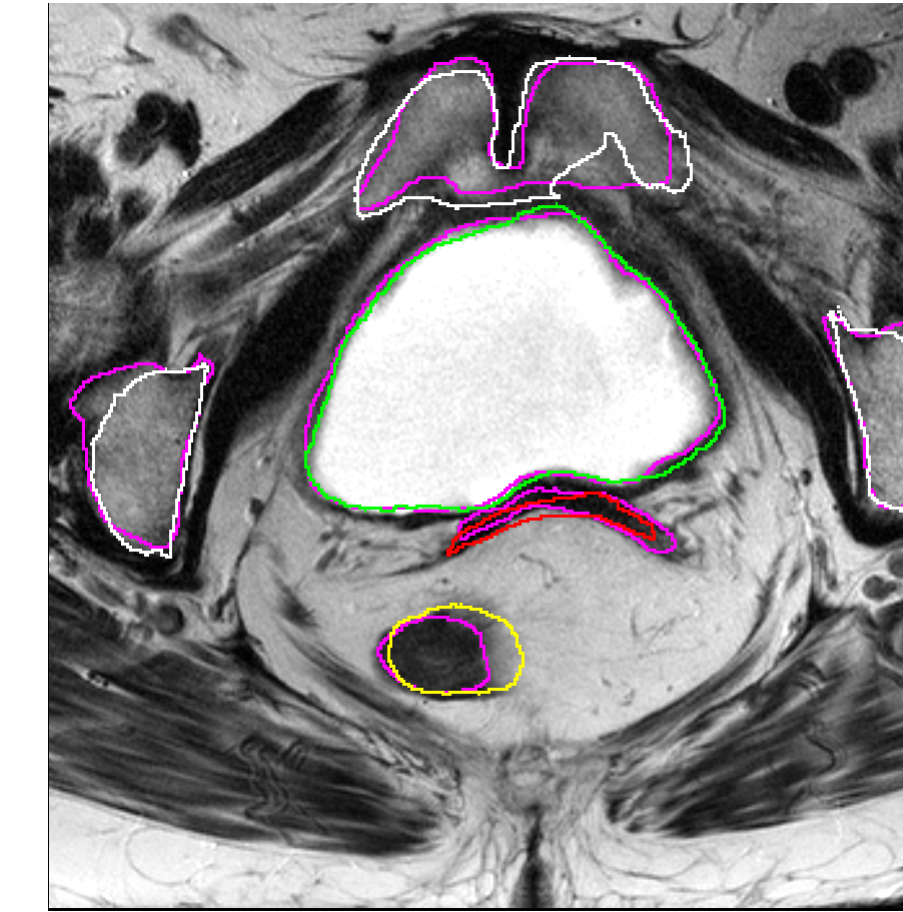


Fig. 11: Final result after fusion process to get one label per organ.

3D Visualization

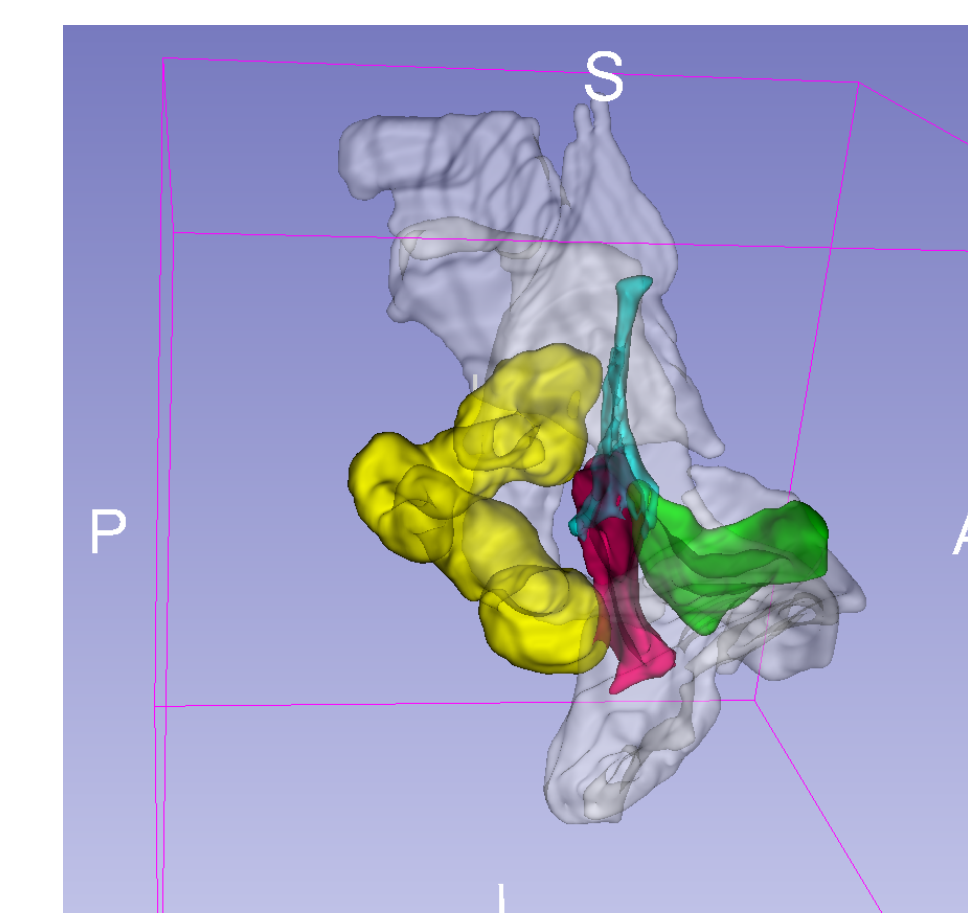


Fig. 12: 3D visualization of pelvic floor created from labeled sagittal data.

In the figure above, "3D Slicer (Slicer)" [1] is used as visualization software to display 3D models of important pelvic organs. After labeling image features in multiple slices for a specific orientation, Slicer uses contour interpolation techniques in order to create a volume from the 2D outlines. This allows to make all voxels other than labeled ones transparent. Moreover, the doctor can use the software to rotate and zoom the 3D semi-transparent, volumetric image.

Alternative Approaches

MAS techniques have been used to process pelvic floor MRI in [2]. The authors of that study used different implementation of MAS steps, e.g. LOP-STAPLE algorithm instead of JLF for the fusion process. The method was then applied to a manually segmented data set of MR images in axial view from 18 patients and tested on one new patient. The robustness of their technique, if applied to a more generic data set, is not clear. One of the goals of our study is to create a MAS technique that can be robustly used to automatically segment the pelvic floor structures and synthetic implants on MR images of all 3 orientations.

Applying the MAS methodology is only one approach to automatically segment pelvic floor organs and synthetic implants. Another possible technique is the application of neural networks to perform the same tasks. With manually labeled data, one can train a neural network to recognize these important features in an arbitrary MRI slice. Our research group is currently working on this alternative approach as well. Moreover, we are open to ideas and suggestions to improve our work.

Challenges & Future Work

The results illustrated in this poster only include the segmentation of important pelvic floor organs. We have not addressed automatic segmentation of synthetic implants and this topic remains open for future research. Moreover, the propagated labels on Fig. 10 are labels from the same patient. Taking one slice as the fixed slice, one can use the closest 4 adjacent slices to set up a toy problem. In other words, the labels on Fig. 10 correspond to variations of pelvic floor organs within the same patient. The reason this was done was due to large variability between inter-patient labels. Due to the small data set of patients, this large variability can be troublesome so intra-patient labels were utilized. Similarly, deep learning approaches require large amount of training data. Therefore, a small data set prevents further study of automatic segmentation of pelvic floor organs. Since a small data set is a bottleneck for our research, we are currently investigating methods of data augmentation to create synthetic data from the limited patient data. We are open to ideas and suggestions to improve our work.

References

- [1] 3D Slicer, www.slicer.org.
- [2] Alireza Akhondi-Asl et al. "A logarithmic opinion pool based STAPLE algorithm for the fusion of segmentations with associated reliability weights". In: *IEEE transactions on medical imaging* 33.10 (2014), pp. 1997–2009.
- [3] Brian B Avants, Nick Tustison, and Gang Song. "Advanced normalization tools (ANTS)". In: *Insight j* 2 (2009), pp. 1–35.
- [4] Brian B Avants et al. "Symmetric diffeomorphic image registration with cross-correlation: evaluating automated labeling of elderly and neurodegenerative brain". In: *Medical image analysis* 12.1 (2008), pp. 26–41.
- [5] Juan Eugenio Iglesias and Mert R Sabuncu. "Multi-atlas segmentation of biomedical images: a survey". In: *Medical image analysis* 24.1 (2015), pp. 205–219.
- [6] Gaurav Khatri et al. "Postoperative imaging after surgical repair for pelvic floor dysfunction". In: *Radiographics* 36.4 (2016), pp. 1233–1256.
- [7] Ingrid Nygaard et al. "Prevalence of symptomatic pelvic floor disorders in US women". In: *Jama* 300.11 (2008), pp. 1311–1316.
- [8] Aparna D Shah et al. "The age distribution, rates, and types of surgery for pelvic organ prolapse in the USA". In: *International Urogynecology Journal* 19.3 (2008), pp. 421–428.
- [9] Guorong Wu et al. "A generative probability model of joint label fusion for multi-atlas based brain segmentation". In: *Medical image analysis* 18.6 (2014), pp. 881–890.